Journal of Alloys and Compounds, *185* (1992) 25–34
JALCOM 218

Structural and magnetic properties of non-equilibrium b.c.c. nickel prepared by leaching of mechanically alloyed $Ni_{35}Al_{65}$

E. Ivanov*, Salah A. Makhlouf, K. Sumiyama, H. Yamauchi and K. Suzuki
Institute for Materials Research, Tohoku University, Sendai 980 (Japan)

G. Golubkuva
Institute of Solid State Chemistry, 630091 Novosibirsk-91, Derzhavina 18 (Russia)

(Received October 28, 1991)

Abstract

Mechanically alloyed nickel aluminide of the composition $Ni_{35}Al_{65}$ retains its b.c.c. (B2) structure after being treated with 20% KOH solution by which at least five-sixths of the Al atoms are removed. X-ray diffraction, transmission electron microscopy, high pressure differential thermal analysis and magnetization measurements were carried out for both as-milled and leached alloys. The b.c.c. nickel is a strong paramagnet and not stable above 470 K: it transforms to the ferromagnetic f.c.c. nickel at high temperatures.

1. Introduction

Amorphous and metastable materials prepared by rapid quenching, sputtering, ion beam irradiation and mechanical alloying (MA) have revealed quite interesting chemical properties which are useful for electrodes, corrosion-resistant materials and catalysts. The Raney catalyst is usually made by leaching a non-noble component from host nickel alloys. The MA technique has several advantages over the conventional pyrometallurgical method of Raney nickel synthesis because MA allows the production of metastable Ni–Al alloys and intermetallic compounds in a wide concentration range in powder form [1, 2] and these alloys and compounds can react with basic solutions giving Raney nickel catalysts with high catalytic activity and selectivity depending on the conditions of the MA process [3].

The leaching treatment of Al–Ni alloys by alkaline solutions leads to removal of the major portion of the aluminium and retains 'skeleton nickel' catalyst. During leaching of equilibrium intermetallic Ni_2Al_3 no intermediate phases with lower aluminium content are formed [4]. However, a recent transmission electron microscopy (TEM) study of the leaching process of a

*On leave from the Institute of Solid State Chemistry, 630091 Novosibirsk-91, Derzhavina 18, Russia.

0925-8388/92/$5.00

thin Ni_2Al_3 foil showed formation of intermetallic NiAl and the texture of the nickel catalyst during propagation of the reaction front in the Ni_2Al_3 crystals. Small-angle diffraction study after low temperature leaching of Ni_2Al_3 proved that the intermediate 'Ni_2Al_3 skeleton' forms relatively large particles (about 60 nm) [5]. Since we have briefly reported the formation of an apparent b.c.c. nickel structure during the leaching of highly defective mechanically alloyed $Ni_{35}Al_{65}$ [6], this paper deals with the characteristics of b.c.c. nickel through X-ray diffraction, differential thermal analysis (DTA), TEM and magnetization measurements.

2. Experimental details

Pure elemental powders of nickel ('carbonyl' type) and aluminium were mixed in an argon glove box to give a composition of $Ni_{35}Al_{65}$. The powder mixture was sealed in a stainless steel vial with the volume of 200 cm^3 together with stainless steel balls 8 mm in diameter. The ball-to-powder weight ratio was 10:1. The MA treatment was carried out in a planetary ball mill with a rotation speed of 700 rev min^{-1} until the crystal structure of the samples was identified as the B2 type. The samples were then treated in 20 wt.% KOH solution at about 370 K in order to leach away aluminium from the milled B2 alloy. The chemical composition of both as-milled and leached samples was determined by conventional chemical analysis and electron probe microanalysis (EPMA). These specimens were characterized by X-ray diffraction, TEM (JEOL EX2000) and DTA at 2.0 MPa of hydrogen gas. A conventional vibrating-sample magnetometer was employed to measure the magnetization between 290 and 770 K in magnetic fields up to 16 kOe and a torsion balance magnetometer to measure the magnetization between 4.2 and 290 K in magnetic fields up to 17 kOe.

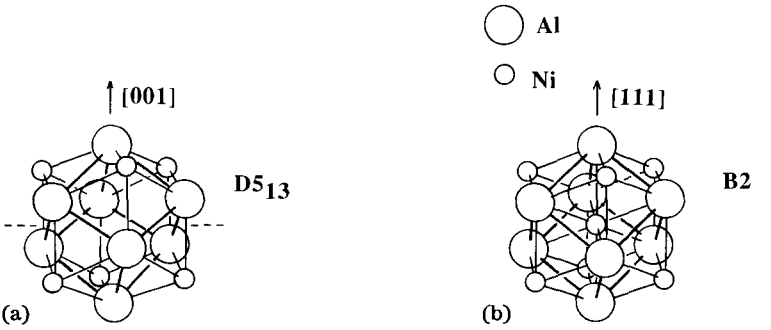

Fig. 1. Comparison of Ni_2Al_3 and NiAl structures [8]. (a) Pseudocubic cell (——) surrounded by neighbouring body-centred Ni atoms and – – –, the missing plane of Ni atoms. (b) B.c.c. cell (CsCl structure) and neighbouring cells (——).

3. Results and discussion

3.1. Structure

The composition of $Ni_{35}Al_{65}$ is close to stoichiometric Ni_2Al_3 ($Ni_{40}Al_{60}$). The structure of Ni_2Al_3 ($D5_{13}$) is closely related to that of NiAl (B2), *i.e.* the former is a deformed type of the latter and derived by replacing one-third of the Ni atoms with completely ordered vacancies in the (111) plane of the NiAl structure as shown in Fig. 1. Since shear displacement and layer-by-layer mixing during the MA process lead to the formation of the NiAl (B2) solid solution, the homogeneity range of NiAl becomes wider, from the equilibrium 45–59.2 at.% Ni to the metastable 35–60 at.% Ni [1], and the concentration ranges of disordered Ni_2Al_3 and NiAl phases overlap. Recently

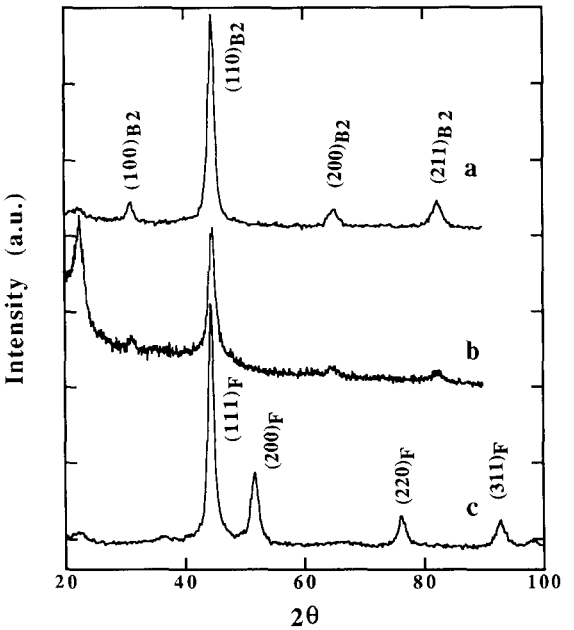

Fig. 2. X-ray diffraction patterns of as-milled $Ni_{35}Al_{65}$ (curve a), leached nickel (curve b) and leached nickel after annealing at 770 K (curve c). The diffraction peak at around $2\theta = 22°$ is due to oxide compounds.

TABLE 1

Comparison of the structural parameters of MA $Ni_{35}Al_{65}$, leached nickel and stoichiometric NiAl intermetallic compound

Sample	Lattice parameter (nm)	Particle size (nm)	R.m.s. strain $<\epsilon^2>^{1/2}$
MA $Ni_{35}Al_{65}$	0.286 ± 0.001	12	7.94
Leached Ni	0.286 ± 0.001	11	8.77
NiAl	0.2882	–	–

disorder transformation has been observed in Ni_2Al_3 after 400 keV Kr^+ ion irradiation at 20 K [7]. The same process can be expected at ambient temperatures in mechanically alloyed intermetallics.

Figure 2 shows X-ray diffraction patterns of as-milled $Ni_{35}Al_{65}$ and leached nickel before and after annealing at 770 K under 2.0 MPa H_2 gas pressure for 1 h. The B2-type order phase has a lattice constant of 0.286 nm. Leached nickel made from MA $Ni_{35}Al_{65}$ exhibits some structural peculiarities. The leaching of Al atoms from $Ni_{35}Al_{65}$ does not induce a significant change in the diffraction pattern even though 60–70% of Al atoms were removed. It should be noted that pyrometallurgical stoichiometric NiAl does not react with an alkaline solution, whereas the defect structure of the MA alloy facilitates the leaching reaction. The lattice parameter, crystalline size and strains do not change (see Table 1) [3] after leaching except for the appearance of a diffuse maximum around the Ni(200) peak. After being annealed at 770 K for 1 h in hydrogen (2.0 MPa) atmosphere the specimen shows the f.c.c. nickel structure without any trace of the B2 type and other Ni–Al intermetallic compounds. This means that almost all the sample was subjected to the leaching reaction.

Figures 3(a) and 3(b) show electron micrographs of as-milled $Ni_{35}Al_{65}$ and leached nickel particles and the corresponding specific-area diffraction (SAD) patterns which show the typical B2 structure. As shown in Fig. 3(c) and its SAD pattern, heating the leached nickel particle in the transmission electron microscope by increasing the electron beam current forms f.c.c. nickel with relatively large crystallites. The aluminium content of the leached samples determined by EPMA was much less than that of milled samples: at least five-sixths of Al atoms were removed during leaching. The remaining aluminium was found in the form of hydroxides and diluted Ni–Al solid solution.

Since hydrogen is formed by decomposition of aluminium hydroxide in the leaching process, conventional DTA or differential scanning calorimetry (DSC) may give a considerable endothermic effect due to the absorption of hydrogen atoms, overlapping an exothermic effect due to the structural transformation. In this experiment therefore we carried out DTA under hydrogen gas atmosphere of 2.0 MPa and studied the transformation process of the leached b.c.c. nickel. As shown in Fig. 4 the DTA traces of leached specimens reveal two exothermic effects. The low temperature peak around 380 K does not correspond to any structural or magnetic transformation because X-ray and magnetization measurements do not show any significant change at this temperature. Similar phenomena have been observed by Koch [8]: the low-temperature DSC peak of MA Ni–Al alloys did not correlate with any change in their properties. The high-temperature peak around 450 K corresponds to the structural transformation from the b.c.c. to f.c.c. structure accompanied by the change in the magnetic properties. The X-ray diffraction pattern shows f.c.c. nickel lines just after heating the specimen to the temperature of the second DTA peak. This structural transformation was completed at 770 K.

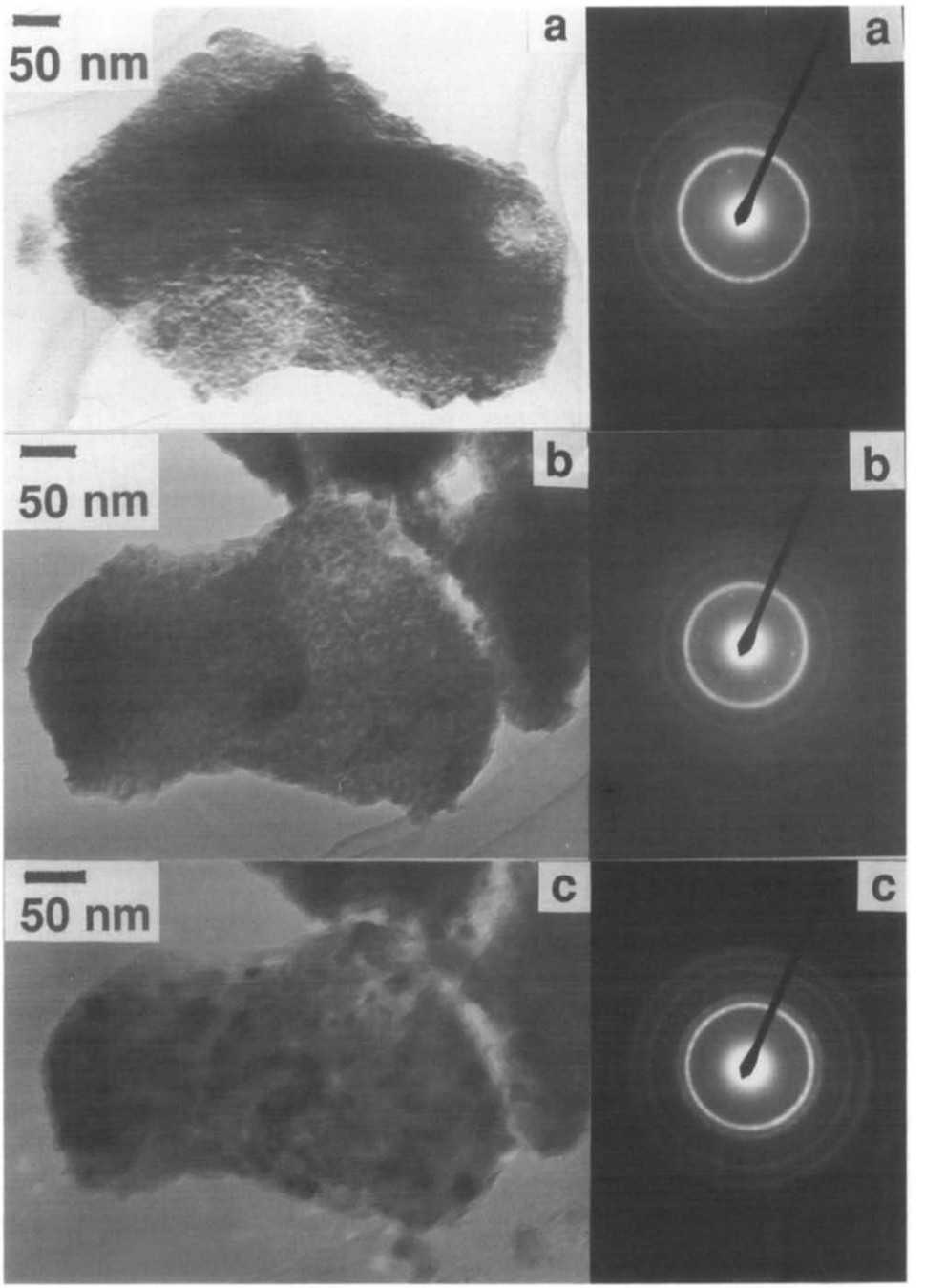

Fig. 3. Transmission electron micrographs and SAD patterns of (a) as-milled $Ni_{35}Al_{65}$, (b) leached nickel and (c) leached nickel after *in situ* annealing by electron beam.

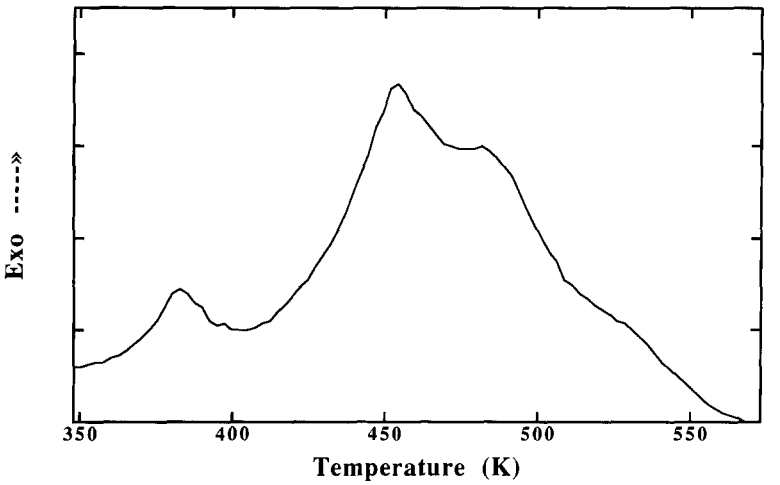

Fig. 4. DTA trace of leached nickel under hydrogen gas atmosphere of 2.0 MPa.

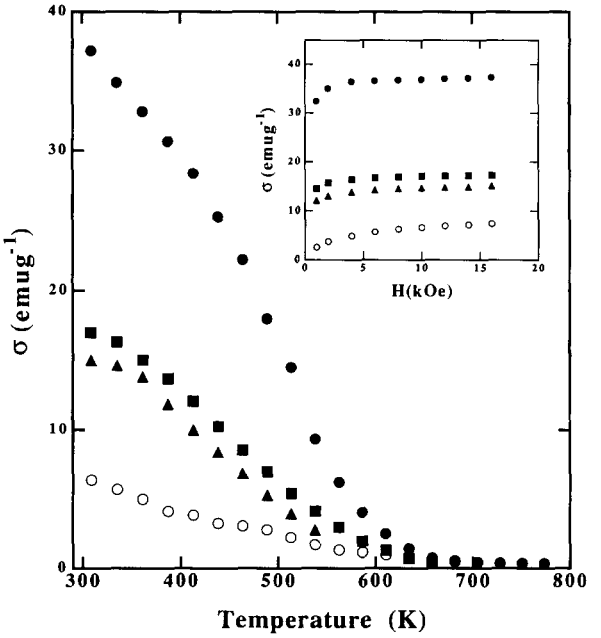

Fig. 5. Temperature dependence of the magnetization σ of leached nickel: ○, σ measured at the heating stage; ▲, ■, ●, σ measured at the cooling stage from 510 K (▲), 630 K (■) and 770 K (●). The inset is the magnetization (σ *vs.* H) curves at room temperature for leached nickel as prepared (○) and cooled from 510 K (▲), 630 K (■) and 770 K (●).

3.2. Magnetic properties

Figure 5 shows the temperature dependence of the magnetization σ of leached nickel specimens between 290 and 770 K in an applied magnetic field H of about 10 kOe. σ is small at 290 K, decreases with increasing

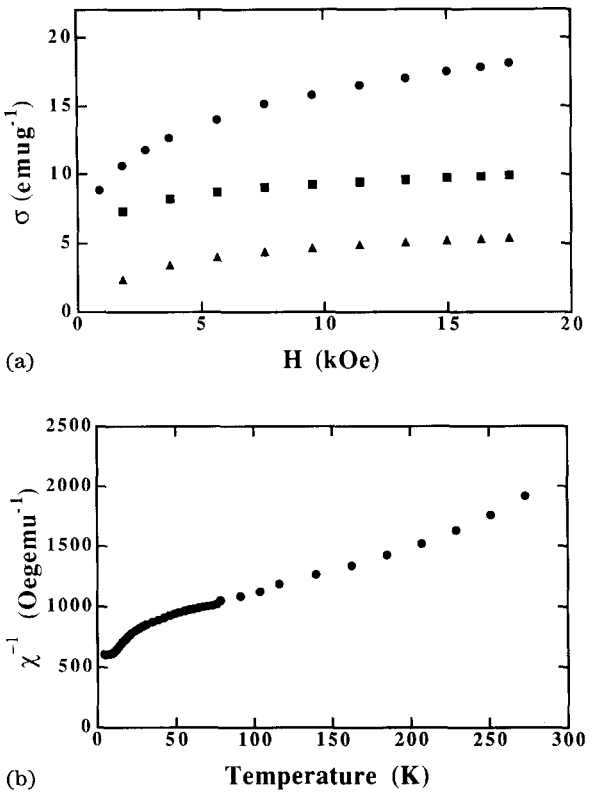

Fig. 6. (a) Magnetization (σ *vs.* H) curves of leached nickel: ●, at 4.2 K; ■, at 77 K; ▲, at 290 K. (b) Thermal variation of the inverse susceptibility χ^{-1} of leached nickel at an applied field of 10 kOe.

temperature and disappears at about 630 K. This indicates the coexistence of ferromagnetic f.c.c. nickel impurities with b.c.c. nickel, as proved by TEM observation. On cooling of the specimen from 770 K σ sharply increases at about 550 K, indicating that b.c.c. nickel transforms to a ferromagnetic f.c.c. phase: the Curie temperature T_c is about 550 K for this ferromagnetic phase and the spontaneous magnetization at room temperature σ_0(RT) is about 36 e.m.u. g^{-1}, which has been estimated from extrapolation of the linear part of the magnetization curve to $H=0$ kOe in the σ *vs.* H plot as shown in the inset of Fig. 5. These values are smaller than $T_c=631$ K and $\sigma_0(\mathrm{RT})=54$ e.m.u. g^{-1} for ferromagnetic f.c.c. nickel [9]. Referring to the concentration dependence of the T_c of bulk and metastable f.c.c. Ni–Al alloys produced by sputtering, the aluminium content in the f.c.c. Ni–Al phase is estimated to be about 6 at.% [10] for $T_c=550$ K. The small σ_0(RT) value suggests the presence of non-magnetic impurities of either aluminium or aluminium hydroxide as previously detected by EPMA and X-ray diffraction. In order to follow this phase transition process we annealed the sample at different temperatures. In the leached specimen annealed for 20 min at 410 K (after

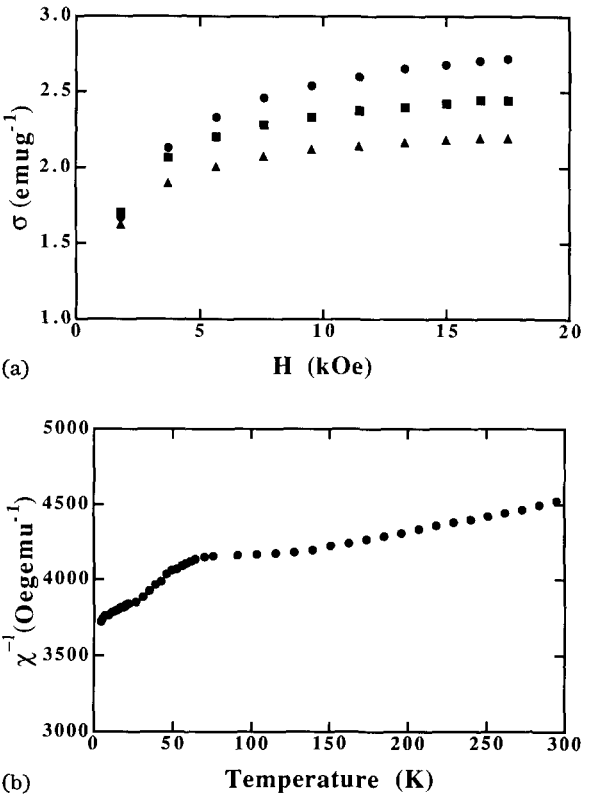

Fig. 7. (a) Magnetization (σ *vs.* H) curves of as-milled $Ni_{35}Al_{65}$: ●, at 4.2 K; ■, at 77 K; ▲, at 290 K. (b) Thermal variation of the inverse susceptibility χ^{-1} of as-milled $Ni_{35}Al_{65}$ alloy at an applied field of 10 kOe.

the first peak in the DTA trace in Fig. 4) no change in the magnetization has been observed. Annealing the sample at 510 K (after passing the second maximum in the DTA trace and below T_c) the magnetization considerably increases: σ_0(RT) is about 15 e.m.u. g^{-1} after cooling down from 510 K. The leached nickel specimen heated to 630 K (Curie point of nickel) and cooled to room temperature shows σ_0(RT) of about 18 e.m.u. g^{-1}. However, the low σ_0(RT) value indicates that the magnetic phase change has not yet been completely accomplished below 630 K.

Figure 6 shows the magnetization curves at room temperature, 77 and 4.2 K, and the temperature dependence of the inverse susceptibility χ^{-1}, for leached nickel specimens measured in an applied field of 10 kOe. The general features of these curves are as follows: (1) the magnetization does not saturate up to $H = 17$ kOe at room temperature and 77 K, and the high-field susceptibility becomes larger at 4.2 K: σ increases monotonically with increasing magnetic field between 10 and 17 kOe; (2) the χ^{-1} *vs.* T plot displays a downward curvature below 50 K. The magnetization $\sigma(H,T)$ at an applied field H and temperature T can be described by the following

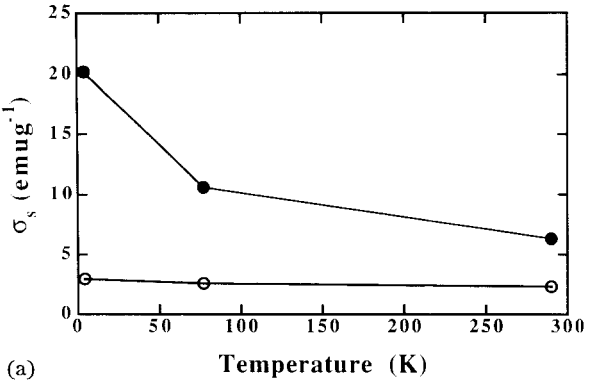

(a)

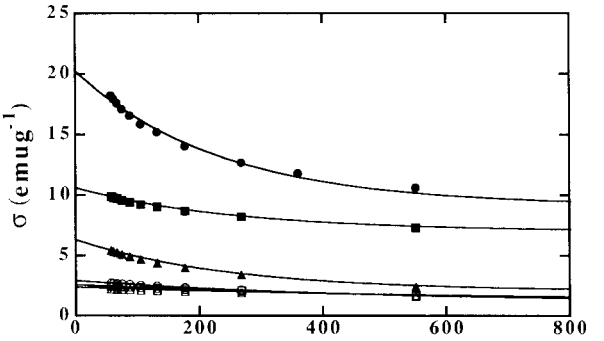

(b)

Fig. 8. (a) Temperature dependence of the saturation magnetization σ_s: ●, leached nickel; ○, as-milled $Ni_{35}Al_{65}$ alloy. (b) σ *vs.* $1/H$ curves of leached nickel (●, ■, ▲) and as-milled $Ni_{35}Al_{65}$ alloy (○, □, △): ●, ○, results at 4.2 K; ■, □, results at 77 K; ▲, △, results at 290 K; ——, the results extrapolated to an infinite field.

formula:

$$\sigma(H,T) = \sigma_o(H,T) + \chi(H,T)\, H \tag{1}$$

Here σ_o (H,T) is attributed to the ferromagnetic impurities of nickel-rich f.c.c. alloys present in the leached nickel specimen and roughly independent of temperature. The increase in $\sigma(H,T)$ with decreasing temperature and the pronounced high-field susceptibility at 4.2 K is attributable to the b.c.c. nickel phase. According to recent band theoretical calculation [11], the b.c.c. nickel should be a paramagnet and it becomes ferromagnetic as its atomic radius expands above a critical value r_c. Since the atomic radius of the present b.c.c. nickel is smaller than r_c, it is a strong paramagnet. Therefore the Curie–Weiss type of temperature dependence of $\chi(H,T)$ gives rise to the rapid increase in $\sigma(H,T)$, in particular at low temperatures. Although the Curie–Weiss law is satisfied in a very wide temperature range ($T = 50$–250 K), the heterogeneity of the sample, namely the presence of both ferromagnetic

and non-magnetic impurities, makes it difficult to estimate the effective magnetic moment per Ni atom for the b.c.c. nickel phase.

As shown in Fig. 7, the magnetizations at room temperature, 77 and 4.2 K for the as-milled $Ni_{35}Al_{65}$ are one order of magnitude smaller than those for the leached nickel, particularly at low temperatures, where they also do not easily saturate in applied fields up to 17 kOe. As shown in Fig. 7(b) the temperature dependence of the inverse susceptibility χ^{-1} in an applied magnetic field of about 10 kOe also displays a downward curvature below 75 K.

Figure 8(a) shows the temperature dependence of the saturation magnetization σ_s for both the as-milled $Ni_{35}Al_{65}$ and the leached b.c.c. nickel, estimated from extrapolating the σ values to infinite field as shown in Fig. 8(b). The temperature-independent behaviour of σ_s for the as-milled sample is due to the ferromagnetic impurities, while the pronounced increase in σ_s with decreasing T for the leached nickel indicates the strong enhancement of the magnetic moment.

In conclusion, X-ray diffraction, TEM, high pressure DTA and magnetization measurements of nickel-rich Ni–Al alloy produced by MA and KOH leaching indicate that this alloy is mainly b.c.c. (or of the B2 type) and a strong paramagnet. After annealing above 470 K, the b.c.c. nickel phase transforms to the ferromagnetic f.c.c. phase.

Acknowledgments

The authors wish to thank Professor T. Masumoto and Dr. K. Aoki for supporting the DTA measurements.

References

1 E. Ivanov, T. Grigorieva, V. Boldyrev, A. Fasman, S. Michailenko and O. Kalinina, *Mater. Lett.*, *7* (1988) 51.
2 E. Ivanov, *Proc. Indian Natl. Sci. Acad. Part A*, *55*(5) (1989) 739.
3 A. Fasman, S. Michailenko, O. Kalinina, E. Ivanov and G. Golubkova, *5th Int. Symp. on Scientific Bases for the Preparation of Heterogeneous Catalysts, Louvain-les-Neuve, September 3–6, 1990.*
4 R. Salloulas and V. Trambouse; *Bull. Soc. Chim. Fr.*, *5* (1964) 985.
5 G. D. Ulianova, Dissertation, Kiev University, 1972, (in Russian).
6 E. Ivanov, G. Golubkova and T. Grigorieva, *Reactivity Solids*, *8* (1990) 73.
7 M. Nastasi, *J. Less-Common Met.*, *168* (1991) 91.
8 C. C. Koch, *J. Non-Cryst. Solids*, *117–118* (1991) 670.
9 H. Gengnagel and A. Arrott, *J. Appl. Phys.*, *39* (1968) 669.
10 K. Sumiyama, Y. Hirose and Y. Nakamura, *Phys. Status Solidi A*, *114* (1989) 693 and references cited therein.
11 V. L. Moruzzi, P. M. Marcus, K. Schwarz and P. Mohn, *Phys. Rev. B*, *34* (1986) 1784.